STUDY OF RE-ENTRY GUIDANCE FOR ORBITAL RECOVERY AND ROCKET FIRST-STAGE RECOVERY

Shuichi Matsumoto [(1)], Hisaaki Arai [(1)], Tomohiko Sakai [(1)]

[(1)]Japan Aerospace Exploration Agency, 2-2-1 Sengen, Tsukuba, Ibaraki, Japan, matsumoto.shuichi@jaxa.jp

ABSTRACT

For new space transport missions such as orbital recovery from Low Earth Orbit (LEO) and the rocket first-stage recovery, accurate re-entry guidance has become increasingly important. We have analysed the characteristics and issues comparing orbital recovery and rocket first-stage recovery.

This paper describes the difference between re-entry guidance for orbital recovery and rocket first-stage recovery, the issues of the re-entry guidance for rocket first-stage recovery, and the method to solve the issue.

1 INTRODUCTION

Accurate re-entry guidance has become increasingly important for space transport missions, such as orbital recovery from Low Earth Orbit (LEO) and the recovery of the first stages of rockets. The Japan Aerospace Exploration Agency (JAXA) has realized several orbital recovery missions, such as the Orbital Re-entry Experiment (OREX)[1],[2], the HAYABUSA re-entry capsule[3], and the HTV Small Re-entry Capsule (HSRC)[4]. The OREX and HAYABUSA re-entry capsules flew ballistic trajectories without re-entry guidance, whereas HSRC flew with re-entry guidance. The recovery accuracy of OREX was 100 km and those of HSRC is 10 km. However, a practical capsule recovery system needs an accuracy of 1 km to ensure a landing on mainland Japan. Thus, our study aimed to realize a re-entry guidance system with 1 km accuracy[6].[8].

JAXA also has been studying recovery missions for he rocket's first-stages based on re-entry guidance using aerodynamic force until the start of the final engine burn. Issues related to this re-entry guidance type differ from those associated with orbital recovery. Our study concentrated on re-entry guidance for rocket first-stage recovery, we have been investigating re-entry guidance for the rocket first-stage recovery because. aerodynamic re-entry can reduce fuel consumption.

This paper demonstrates the difference between re-entry guidance for orbital recovery and rocket first-stage recovery. This paper also describes the issues facing re-entry guidance for rocket first-stage recovery.

2 RE-ENTRY GUIDANCE FOR ORBITAL RECOVERY

2.1 Re-entry Missions of Orbital Recovery in Japan

Japan's first orbital re-entry mission was the Orbital Re-entry Experiment (OREX). OREX was launched by an H-II rocket in 1994, executed a deorbit maneuver into the Earth's atmosphere, and performed ballistic flight during the re-entry phase[5]. Since OREX flew without re-entry guidance,

the recovery accuracy of OREX was 100 km. The photograph and flight result are shown in Figures 1 and 2.

Japan's first orbital re-entry mission with re-entry guidance was the HTV Small Re-entry Capsule (HSRC), which was integrated into an H-IIA transfer vehicle (HTV) and Japan's first re-entry capsule was developed to return samples from the International Space Station (ISS). The capsule was about 0.8 m in diameter, making it the world's smallest vehicle to re-enter from low Earth orbit (LEO). On November 11, 2018, JAXA succeeded in its HSRC re-entry flight demonstration[4]. Figure 3 shows the photograph of the recovery of HSRC after its re-entry flight. Figure 4 shows the re-entry flight results. Since the GPS receiver on HSRC didn't work during HSRC flight, the navigation error of HSRC didn't be corrected by GPS navigation and the re-entry error caused by the navigation error remained.

Figure 1 Photograph of OREX[5]

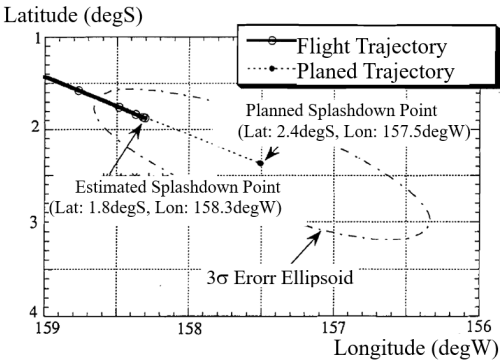

Figure 2 Splashdown Area of OREX[5]

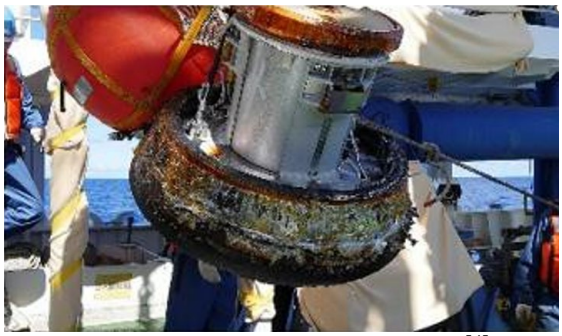

Figure 3 Recovery of HSRC[4]

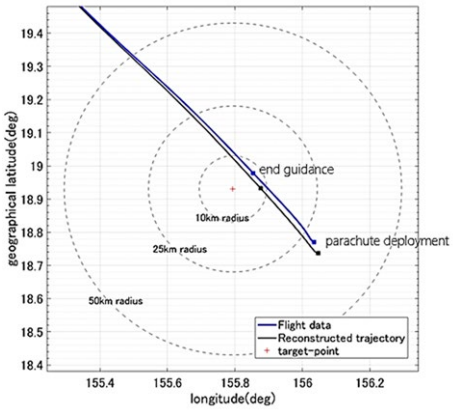

Figure 4 Splashdown Area of HSRC[4]

2.2 Outline of Real-time Prediction Guidance Using Numerical Integration

We proposed the real-time prediction guidance using numerical integration (REP-NI Guidance) for re-entry spacecraft in References [7] and [8] and this re-entry guidance was installed to HSRC and tested on HSRC as the re-entry guidance method during the re-entry flight.

REP-NI Guidance is in the form of an explicit guidance law using real-time numerical integration to predict the accurate range during reentry flight. Figure 5 shows its schematic diagram. The basic concept of the guidance of orbital re-entry is that re-entry guidance changes the vertical component of aerodynamic force by bank angle, altering the upcoming aerodynamic acceleration profile to which re-entry vehicles is subject. Since this guidance method calculates flight range accurately in flight by numerical integration following with precise re-entry flight dynamics, it is very accurate and robust for errors in re-entry flight. Although range prediction using numerical

integration includes such advantages, the heavy computational load involved prevents its use for reentry guidance. We thus improved the range prediction algorithm to reduce computational load while retaining guidance accuracy and showed the feasibility of applying real-time prediction guidance using numerical integration for the re-entry flight in References [7] and [8].

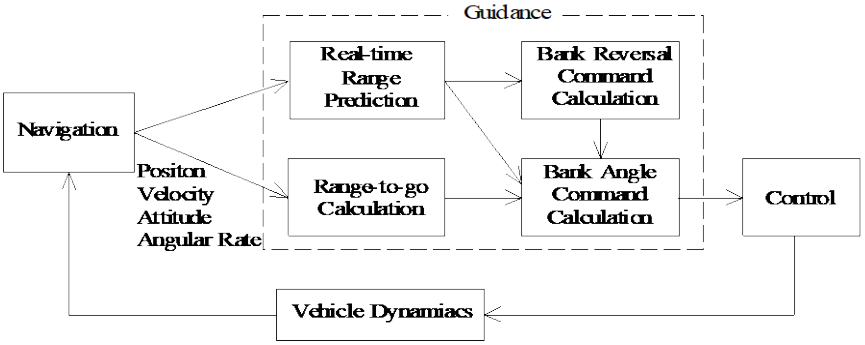

Figure 5 Schematic Diagram of Real-time Prediction Guidance using Numerical Integration (REP-NI Guidance)

The range guidance equation for REP-NI Guidance is shown in Eq. (1) and its bank angle command is shown in Eq. (2). Range predictions in Eqs. (1) and (2) are performed by numerical integration during re-entry flight phases. The sensitivity coefficient of the L/D change for flight range is made using two range predictions for different bank angles. The amount of correction is calculated by multiplying the sensitivity coefficient and range error.

$$(L/D)_C = (L/D)_0 - \frac{\partial (L/D)_0}{\partial R_0} \cdot (R_0 - R_{ref}) = (L/D)_0 - \frac{\Delta (L/D)}{R_1 - R_0} \cdot (R_0 - R_{ref}) \quad (1)$$

$$\cos(\phi_c) = \cos(\phi_0) - \frac{(\cos(\phi_0 + \Delta\phi) - \cos(\phi_0))}{R_1 - R_0} \cdot (R_0 - R_{ref}) \quad (2)$$

where
$(L/D)_0$, $(L/D)_C$: L/D command at previous guidance cycle and at present cycle
$\Delta(L/D)$: Increment of L/D for increment of bank angle $\Delta\phi$
ϕ_0, ϕ_c: Bank angle commend at previous guidance cycle and at present cycle
$\Delta\phi$: Increment of bank angle for calculation of sensitivity matrix
R_{ref}: Range to target point from present point
R_0: Predicted range to target point when spacecraft flies at the bank angle of previous guidance cycle
R_1: Predicted range to target point when spacecraft flies at the bank angle $(\phi_0 + \Delta\phi)$

2.3 Simulation Results of Orbital Re-entry Using REP-NI Guidance

Figure 7 shows one of the Monte Carlo simulation results of orbital re-entry using REP-NI guidance, in-orbit alignment, and IMU-GPS-Drag Measurement (DM) navigation.[8] The error factors using this simulation are shown in Table 1. In the simulation, there are errors caused by wind errors whose error model are shown in Fig.6. After applying REP-NI, in-orbit alignment, and IMU-GPS-DM integrated navigation, upper-level wind error is the only major factor affecting re-entry guidance error. To improve the re-entry guidance under wind errors, we can apply the method using upper-wind information measured by a ground site, which is uploaded to the capsule spacecraft before its re-entry flight. The issue with this method is that during real flight operation, the upper-level wind may change while the spacecraft flies from the time when the spacecraft has had upper-level wind information uploaded to the time when it reaches the target area. We have been studying this method for re-entry future missions.

Table 1 Error Factors using Re-entry Guidance Analysis

Error Factors	Error (3σ)
Down Range Direction	±100 km
Cross Range Direction	±4 km
Inertial Velocity	±1 m/s
Flight Path Angle	±0.06 º
Flight Direction Angle	±0.04 º
Position	±45 m
Velocity	±0.09 m/s
Attitude	±0.5 º
Acceleration Bias	±130 G
Acceleration SF	150 μG/G
Gyro Bias Drift	±0.096 deg/hr
Gyro Rate Noise	0.0008 º/s$^{0.5}$
Misalignment	30 arcsec
Altitude 10-30 km : ±10% 60-80 km : ±50% 100-120 km: ±70%	
Lift Coefficient	±25 %
Drag Coefficient	±25 %
Vehicle Weight	±1 ton
Wind Error (East, West, North, South)	See Figure 6

Error Factors		Error (3σ)
GPSR Error	Pseudo-range Bias	±15.3 m
	Pseudo-range Noise	9.9 m
	Clock Frequency Noise	9.0 m/s
	Blackout : Altitude from 95 to 40 km	
STT Error	Pointing Direction Bias	±0.01 º
	Random (cross bore-sight axis)	0.003 º
	Random (bore-sight axis)	0.015 º

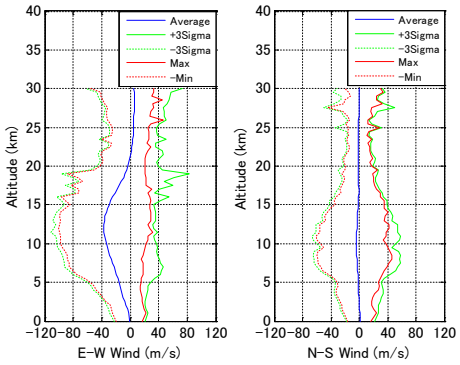

Figure 6 Upper-level Wind Measured at Tanegashima Space Center

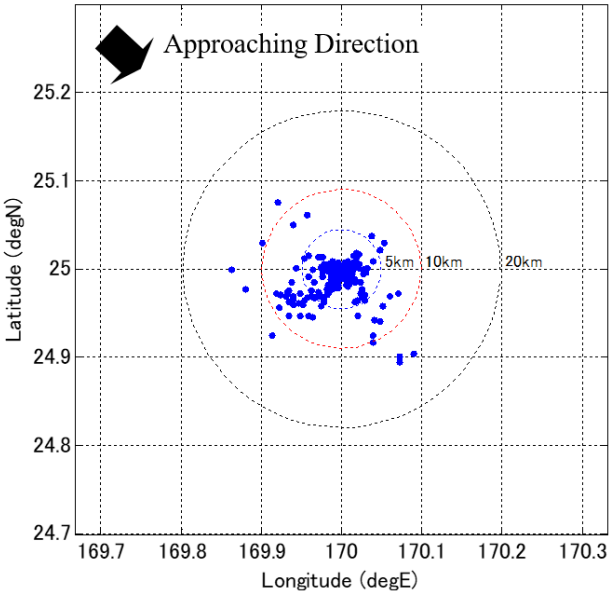

Figure 7 Monte Carlo Simulation Result of Re-entry Guidance using REP-NI Guidance, in-orbit and IMU-GPS-DM Integrated Navigation

3 RE-ENTRY GUIDANCE FOR ROCKET FIRST-STAGE RECOVERY

3.1 Rocket First-stage Recovery Missions in Japan

JAXA studied rocket first-stage recovery missions in the late 1990s, as described in reference [9]. The concept was a two-stage-to-orbit (TSTO) mission in which a rocket's first-stage flies forward after the first and second stages separate, then lands on a ship at the planned landing point of the rocket's first-stage. [9] Figure 8 shows the mission concept. A study from the late 1990s used a closed-form re-entry guidance similar to that used for the Space Shuttle.

Although a rocket' first-stage can fire its engine to control the flight trajectory, aerodynamic force is still important to change flight a in certain regions to reduce fuel consumption. A rocket first-stage with re-entry guidance uses aerodynamic force until the start of the final engine burn. Issues of rocket first-stage recovery differ from those of orbital recovery and are followings.

(1) Short time of re-entry guidance using aerodynamic force.
(2) High dynamics pressure during re-entry flight.
(3) How to combine aerodynamics re-entry guidance and guidance using propulsion.

Since using aerodynamic re-entry guidance might reduce the fuel consumption of rocket first-stage recovery, we have been investigating re-entry guidance for rocket first-stage recovery missions. JAXA also has been developing rocket landing experiment vehicles. RV-X (Reusable Vehicle eXperiment)[11] and CALLISTO (Cooperative Action Leading to Launcher Innovation in Stage Toss-back Operations)[12] which is a collaboration development mission between, CNES, DLR, and JAXA.

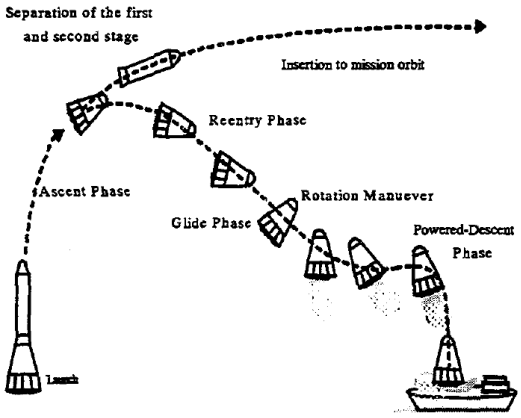

Figure 8 A rocket first-stage recovery mission studied in late 1990s in JAXA [8]

3.2 Characteristic of Flight Trajectory of Rocket First-stage re-entry

Figure 9 shows the Comparison of characteristics of flight trajectory between orbital re-entry and rocket first-stage re-entry. A typical flight trajectory for orbital re-entry is shown in Fig.9 with red and purple dashed lines. Since an aerodynamic heat of orbital re-entry is very severe, the flight path angles of orbital re-entry are small. Regarding of the flight trajectory in Fig. 9, the flight path angle is 2^{o}. In the range of such flight path angle, dynamic pressures of orbital re-entry are much smaller than those of rocket first-stage re-entry as shown in Fig.9 (f). Aerodynamic acceleration can be reduced by using lifted re-entry of orbital re-entry during the re-entry phase.

A typical flight trajectory of rocket first-stage re-entry is shown in Fig.9 with a light bule bold lines. As a reference, a typical flight trajectory of the first-stage of H3 rocket after the first and second separation is shown in Fig.9 with a bule lines. From the constraint for a rocket second stage

to reach an orbit around the Earth, the flight path angles of the initial point of a rocket first-stage re-entry, which is a point of the first and second stage separation, is much larger than those of orbital re-entry capsules as Fig.9 (e). Since the re-entry flight path angle of rocket first-stage re-entry becomes almost a negative angle to the initial flight path angle, the rocket first-stage dives into atmosphere with a large negative flight path angle. Due to the large negative flight path angle, the dynamic pressure of the first-stage becomes very large compared to those of orbital re-entry as shown in Fig. 9 (f). The dynamics pressure of H3 first-stage re-entry is much larger than the constraint of the dynamic pressure of H3, 50 kPa. Thus the trajectory of rocket first-stage re-entry must be designed considering the constraint of re-entry flight. The light blue line indicated as "1st stage re-entry (RLV)" in Fig.9 is one example of trajectory for rocket first-stage re-entry. Even this trajectory considers the constraint of re-entry, large dynamic pressure is an issue to be solved to realize the rocket first-stage re-entry.

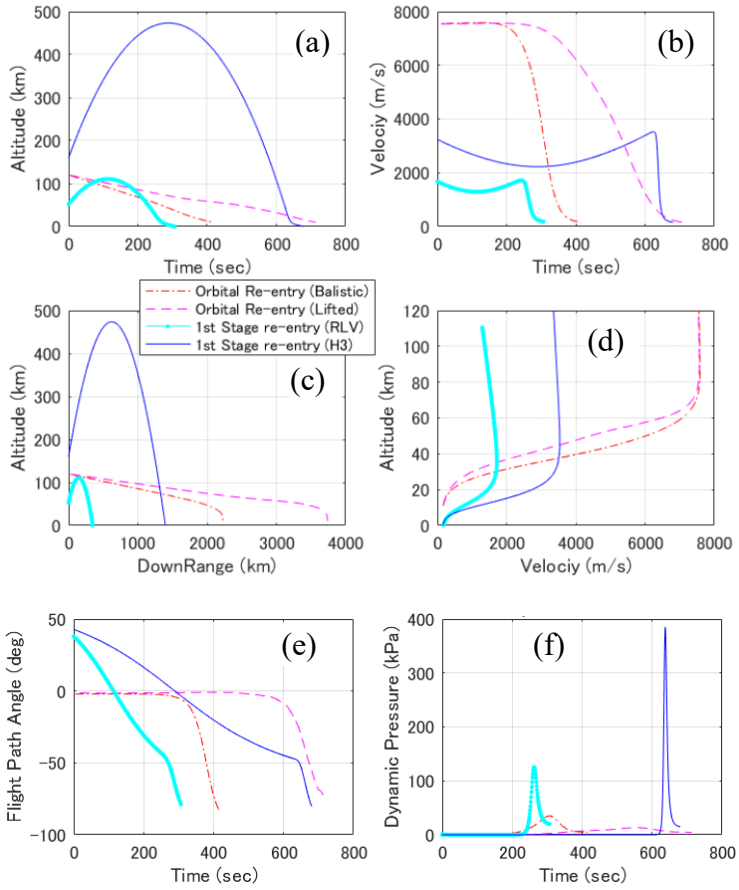

Figure 9 Comparison of characteristics of flight trajectory between orbital re-entry and rocket first-stage re-entry

3.3 Analysis of Flight Trajectory of Rocket First-Stage re-entry

A typical flight trajectory for a rocket's first-stage re-entry mission is shown in Figure 10, which shows four Lift-Drag ratios (L/D) applied during aerodynamic flight phase. We found that their trajectories are almost the same. Figure 11 illustrates the final part of the flight trajectories of the rocket's first-stage re-entry to demonstrate the re-entry guidance capability using aerodynamic force. In Fig.11 we see that the re-entry guidance capability using aerodynamic force is about 10 km using L/D from 0 to 0.3.

As mentioned in the previous section, high dynamic pressure during re-entry flight is a large issue for a rocket's first-stage recovery. Figure 12 shows the dynamic pressure profile of the rocket first state re-entry flight for four different L/Ds to demonstrate the dynamic pressure issue. Although the limitation of the dynamic pressure of current rockets, such as the H3 rocket, is less than 50 kPa, Fig. 12 shows that the dynamic pressure of the rocket's first stage re-entry is 130 kPa for ballistic re-entry (upper left of Fig.12) and is 110 kPa in the case of lifted re-entry whose L/D is 0.3 (lower right of Fig. 12).

The cause of this high dynamic pressure is the trajectory interface between a rocket second stage for orbit insertion and a rocket first-stage returning to the Earth's surface. The flight path angle of the rocket first-stage recovery at the first and second stage separation is about 30^{o} required for the second stage to reach on-orbit. After the separation, the rocket first-stage flies to a maximum altitude according to the law of inertia, returns toward the Earth, and finally enters to the atmosphere with a flight pass angle of -30^{o} or more. Since the angle is fairly steep, the dynamic pressure is rather large.

Figure 13 shows parametric studies of the dynamic pressure of rocket first-stage re-entry. To see the effect of a flight path angle difference on dynamic pressure, a comparison of Fig. 13 (a) and (b) shows that a flight path angle difference of -5^{o} made a maximum dynamic pressure reduction of 30 kPa. To see Comparing Fig. 13 (b) and (c) shows the effect of an altitude at the first and second stage separation, that an increase in altitude increases dynamic pressure. Fig. 13 (d) shows the case in which a re-entry vehicle made a re-entry burn to reduce the velocity before maximum dynamic pressure. In case (d), the maximum dynamic pressure meets the limitation of the dynamic pressure of 50 kPa.

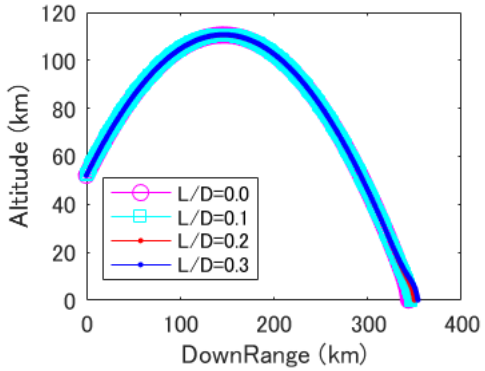

Figure 10 Flight trajectory of rocket first-stage recovery

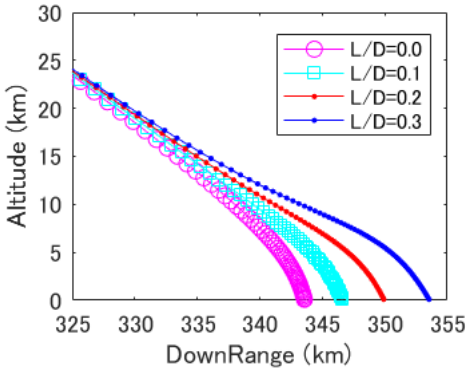

Figure 11 Enlargement of flight trajectory (Final part of the flight trajectory)

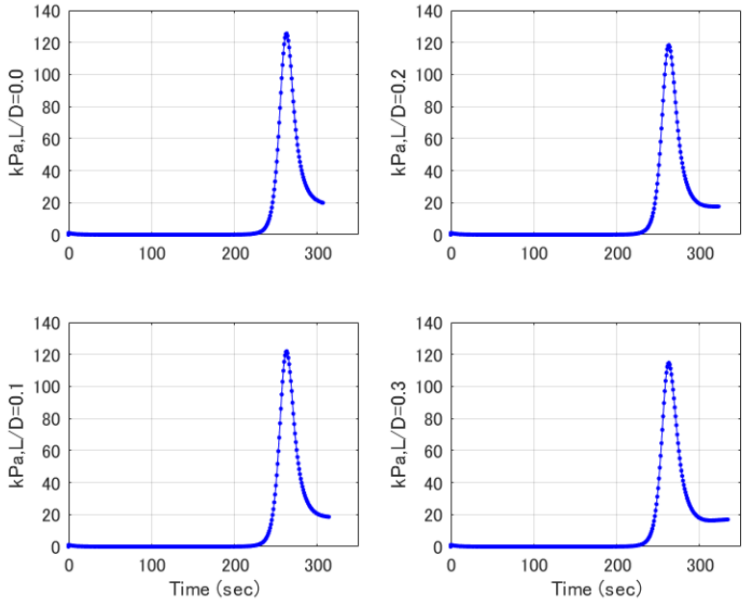

Figure 12 Parametric studies of the dynamic pressure of rocket first-stage re-entry
(Lifted Flight with for four different L/Ds)

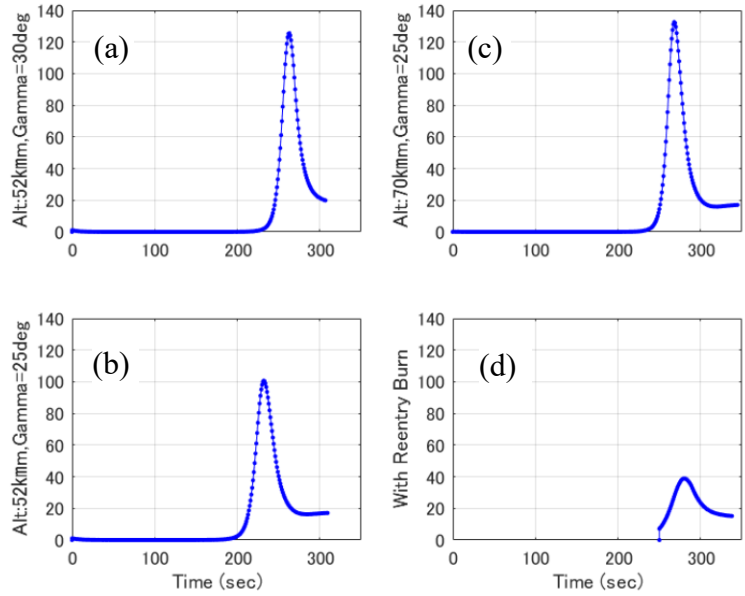

Figure 13 Parametric studies of the dynamic pressure of rocket first-stage re-entry
(Altitude, Flight path angle (Gamma), and with re-entry burn)

3.4 Re-entry Guidance for Rocket First-stage Recovery Missions

Since propulsion powered flight with aerodynamic forces and lifted aerodynamic flight are required for rocket first-stage recovery missions, the combination of powered flight guidance and lifted flight guidance in atmosphere is required for rocket first-stage recovery missions. Thus we have been studying the combination the convex optimization technique[9] for power fight guidance and the Real-time Prediction Guidance using Numerical Integration (REP-NI Guidance) for lifted aerodynamic flight.

4 CONCLUSIONS

This paper analyses the characteristics and issues of orbital recovery and rocket first-stage recovery. JAXA has restarted research on rocket first-stage recovery missions and related techniques to realize a rocket first-stage re-entry and landing. We have been applying the convex optimization technique for powered flight, the Real-time Prediction Guidance using Numerical Integration (REP-NI Guidance), and their combination for rocket first-stage re-entr missions.

5 REFERENCES

[1] Akimoto, T., Ito, T., Yamamoto, M., Bando, T., and Inoue,Y., *Orbital Re-entry Experiment (OREX) - First step of space return flight demonstrations in Japan*, Proceedings of 45th IAF International Astronautical Congress, 1994.

[2] Matsumoto, S., Suzuki, H., Izumi, T., Mori, T., Sugano, K., Wakamiya, M., and Mitsui, S., *Evaluation of the Guidance, Navigation and Control System for OREX*, Special Report of National Aerospace Laboratory, SP-24, pp.117-130, 1994.

[3] Yamada, K., Yamada, T., Matsuoka, M., *EDL analysis for "HAYABUSA" Reentry and Recovery Operation*, Proc. of 20th workshop on Astrodynamics and Flight Mechanics, 2010.

[4] Haruki, M., Nakamura, R., Matsumoto, S., Kobayashi, S., Kawashima, I., Aoki, K., Kikuchi, N., *Post-Flight Evaluation of the Guidance and Control for Re-entry Capsule "HSRC"*, Proceedings of 8th European Conference for Aeronautics and Space Sciences (EUCASS)

[5] Matsumoto, S., Kondoh, Y., Nagai, S., Tagai, R., Imada, T., Nakano, E., *Aerodynamic Oscillation and Attitude Control Analysis for Reentry Capsule using OREX Flight Data and Wind Tunnel Data*, Proc. of AIAA SciTech Forum 2016, Guidance, Navigation, and Control Conference, AIAA 2016-1131, 2016.

[6] Matsumoto, S., Kondoh, Y., Imada, T., Sato, N., *Technical Challenges and Study on Guided Reentry Flight for Capsule Spacecraft*, Journal of Space technology and science, Vol.27, No.2, pp.21-30, 2013.

[7] Matsumoto, S., Kondoh, Y., Suzuki, Y., Imada, T., Sato, N., Kobayashi, S., Motoyama, N., *Accurate Real-Time Prediction Guidance Using Numerical Integration for Reentry Spacecraft,* Proc. of AIAA Guidance, Navigation, and Control Conference, AIAA 2013-4646, 2013.

[8] Matsumoto, S., Kondoh, Y., Haruki, M., Imada, T., Kobayashi, S., Motoyama, N., *IMU-DM Integrated Navigation and Terminal Reentry Guidance for Accurate Guided Reentry Flight,* Proc. of AIAA SciTech Forum 2015, Guidance, Navigation, and Control Conference, AIAA 2015-1772, 2015.

[9] Ishijima, Y., Matsumoto, S., and Hayashi, K., *Re-entry and Terminal Guidance for Vertical-Landing TSTO (Two-Stage to Orbit),* Proc. of AIAA Guidance, Navigation and Control Conference 1998, AIAA 98-4120, 1998.

[10] Hisaaki, A., Sakai, S., *Rapid Generation of Navigation-Optimal Trajectories for Planetary Landing via Convex Optimization,* Proc. of AIAA SciTech Forum 2015, Guidance, Navigation, and Control Conference, AIAA 2019-0666, 2019.

[11] Nonaka, S., Ito, T., Inatani, Y., *Technical and Flight Demonstrations for Reusable Launch Vehicle,* Proc. of 30th International Symposium on Space Technology and Science, ISTS-2017-o-3-01, Matsuyama, 2017.

[12] Dumont,E., Ishimoto, S., Illig, M., Sagliano, M., Solari, M., Ecker, T., Martens, H., Krummen, S., Desmariaux, J., Saito, Y., Ertl, M., Klevanski, J., Reimann, B., Woicke, S., Schwarz, R., Seelbinder, D., Markgraf, M., Riehmer, J., Braun, B., Aicher, M., *CALLISTO: current status of the development of key technologies for reusable launch vehicles*, Proc. of 33rd International

Symposium on Space Technology and Science, ISTS-2017-g-13, Oita, 2022.